200812040A

厚生労働科学研究費補助金

医療機器開発推進研究事業

「ＲＮＡ創薬を支援するバイオイメージング技術の確立」に関する研究

平成２０年度　総括研究報告書

研究代表者　浅井　知浩

平成２１（２００９）年　４月

目　　次

厚生労働科学研究費補助金（医療機器開発推進研究事業）
統括研究報告書

ＲＮＡ創薬を支援するバイオイメージング技術の確立（H20-ナノ-若手-007）

主任研究者　浅井 知浩　静岡県立大学大学院薬学研究科講師

研究要旨　small interfering RNA（siRNA）の医療応用を促進するには、疾患部位に必要量の siRNA を送達することを目的とした核酸デリバリーシステムの開発が鍵になる。これまで siRNA ベクターの体内動態は詳細に解析されてきたが、主薬である siRNA 本体の体内動態は未知のことが多い。そこで本研究では siRNA の体内動態を非侵襲的、リアルタイムかつ高感度に解析する技術の確立を目的とし、siRNA の ^{18}F ポジトロン標識体の開発ならびにポジトロン断層法（positron emission tomography; PET）による動態解析技術の構築を目指した。研究計画の初年度である本年度は、siRNA ポジトロン標識体の開発、PET 動態解析、蛍光インビボイメージングによる siRNA 動態解析を実施した。まず本研究に用いる siRNA の配列、ポジトロン標識部位、siRNA とポジトロンの結合様式等の設計を行った。ポジトロンの標識部位は、アンチセンス鎖 3'末端に決定し、共有結合によるポジトロン標識を選択した。次に、標識 siRNA を検出可能な LC/ESI-TOF-MS の分析条件を確立した。また、分取カラムを用いた HPLC 分析条件を確立し、ポジトロン標識 siRNA の分取に成功した。この標識 siRNA が合成中に分解を受けていないことを確認し、インビボ解析への応用が可能であることを明らかにした。実際に調製したポジトロン標識 siRNA をマウスに静脈内投与し、その体内動態の PET 解析を実施した。siRNA 単体とリポソームに搭載した siRNA の体内動態の差異をイメージングすることに成功した。

一方、主薬である siRNA と運搬体であるベクターの体内動態が一致しているか否かを評価していくうえで、リポソームベクターの PET 動態解析方法について検討した。我々が開発したポジトロン標識プローブを用いてリポソームを放射標識し、PET を用いてその体内動態を解析した。また、ポジトロン標識 siRNA の PET 解析データの検証に有用であると考えられる蛍光インビボイメージング法を利用し、蛍光標識 siRNA の体内動態を解析した。近赤外蛍光色素 Alexa750 をアンチセンス鎖 3'末端に結合した siRNA を合成し、蛍光リアルタイムイメージングに用いた。リポソームベクターに搭載した Alexa750 標識 siRNA をマウスに投与し、その体内動態を解析した。そして、得られた蛍光イメージングデータを PET 解析データと比較した。

研究計画初年度の研究事業を当初の計画に沿って遂行し、siRNA 体内動態の PET 解析技術の確立に向けて着実な研究成果が得られた。

A. 研究目的

RNA 干渉は、次世代の医療技術として有望視されており、いわゆる RNA 創薬に関する研究は医療応用に向けて着実に進展している。small interfering RNA（siRNA）の医療応用を促進するには、疾患部位に必要量の siRNA を送達することを

目的とした核酸デリバリーシステムの開発が重要課題といえる。これまでsiRNAの運搬体（リポソーム、高分子ミセル等のベクター）の体内動態は詳細に解析されてきたが、主薬であるsiRNA本体の体内動態は未知のことが多い。そこで本研究ではsiRNAの体内動態を非侵襲的、リアルタイムかつ高感度に解析する技術の確立を目的とし、siRNAの^{18}Fポジトロン標識体の開発ならびにポジトロン断層法（positron emission tomography; PET）による動態解析技術の構築を目指した。本研究の特徴は、1）他の類似技術よりも比較的に高感度なイメージング技術であること、2）ベクターではなく主薬であるsiRNAの動態解析技術であること、3）疾患、標的配列、ベクターによって限定されず応用範囲が広いこと、4）ヒトマイクロドーズ試験への発展性などが挙げられる。

本研究の目標達成によってsiRNAの体内動態データが取得可能となれば、治療効果を予測するうえでもDDS製剤の設計にフィードバックするうえでも貴重な情報が得られることになり、動物を利用したヒトでの有効性・問題点評価に有効であると考えられる。さらにPETは、がん検診でヒトでの使用実績があるうえ、今後はマイクロドーズ試験への応用が期待されており、siRNAのPETによる動態解析は先見性の高い試みとなりうる。3ヶ年計画の研究事業の具体的な検討項目としては、siRNAポジトロン標識体の開発、siRNA体内動態のPET解析技術の確立、蛍光インビボイメージングとの比較、標識siRNAを搭載した各種ベクターの動態解析、病態モデル動物におけるsiRNA動態解析を計画している。

研究計画の初年度である本年度は、siRNAポジトロン標識体の開発、PET動態解析、蛍光インビボイメージングによるsiRNA動態解析を重点的に実施した。

B. 研究方法

（1）siRNAポジトロン標識体の開発

siRNAのアンチセンス鎖3'末端への共有結合によるポジトロン標識を選択した。まずアンチセンス鎖3'末端をアミノ化したsiRNAを北海道システム・サイエンス社に委託して合成した。siRNAの配列はスクランブル（コントロール）配列とした。

siRNAのポジトロン標識は、[^{18}F]-コハク酸イミド誘導体を用いて実施した。この^{18}F誘導体をアミノ化siRNAとホウ素緩衝液中で混合し、室温にて20分間静置して反応させた。なお、ポジトロン放出核種を取り扱う実験は、浜松ホトニクス株式会社中央研究所PETセンターの研究協力を得て実施した。

（2）siRNA分析法の検討

siRNAのセンス鎖、アンチセンス鎖、およびアニーリング後の2本鎖をそれぞれ検出可能なLC/ESI-TOF-MSの分析条件を検討した。まず、コールド（非放射性）の化合物を用いて分析法を確立し、その条件をポジトロン標識siRNAの分析に応用した。HPLCのカラムにはC18 ODSを用い、移動相はTEAAとアセトニトリルとのグラジエント条件とした。ESI-TOF-MS計測時のイオン化では、ネガティブイオン化モードを選択した。

（3）リポソーム化siRNAの調製

カチオン性脂質DOTAPとコレステロールを*t*-ブタノール溶液中で混合し、一晩凍結乾燥した。RNaseフリーのリン酸緩衝液で水和後、リポソームの粒子径をエクストルージョン法にて約100 nmに調整した。ポジトロン標識siRNAとリポソームを室温で20分間インキュベートし、リポソーム化siRNAを調製した。

（4）siRNA体内動態のPET解析

ポジトロン標識siRNA単体ならびに上述のリポソームに搭載したポジトロン標識siRNAの体内動態を解析した。5週齢雄性BALB/cマウスに各サンプルを尾静脈内投与し、簡易型2次元PET装置（planer positron imaging system）を用いて体内動態を解析した。1時間のPET計測終了後にマウスを解剖し、各臓器における放射活性をガンマ

カウンターにて測定した。

(5) ポジトロン標識リポソームの PET 解析

以前に我々が開発した solid-phase transition 法により、リポソームを ^{18}F でポジトロン標識した。標識プローブとしては Stearyl-N2 を用いた。5 週齢雄性 BALB/c マウスにポジトロン標識リポソームを尾静脈内投与し、簡易型 2 次元 PET 装置を用いて体内動態を解析した。1 時間の PET 計測終了後にマウスを解剖し、各臓器における放射活性をガンマカウンターにて測定した。

(6) 蛍光標識 siRNA のインビボイメージング

近赤外蛍光色素である Alexa750 で標識した siRNA を用いて、siRNA 搭載リポソームを調製した。蛍光インビボイメージングの装置としては、Xenogen 社の IVIS® Lumina を用いた。5 週齢雄性 BALB/c マウスに尾静脈内投与し、投与直後より経時的に siRNA の体内動態を観察した。1 時間のイメージング終了後にマウスを解剖し、各臓器における蛍光強度を *ex vivo* にて評価した。

・倫理面への配慮

当該研究に関して、すべての動物実験プロトコールは、所属機関における動物実験委員会による審査・承認を受けている。また、動物愛護の精神にのっとり、実験により派生する恐怖・苦痛をできるかぎり軽減できる方法を選択して用いた。

C. 研究結果

(1) siRNA ポジトロン標識体の開発

siRNA を非放射性の F で標識し(コールドラン)、HPLC 分析を行った結果、標識 siRNA と未反応の siRNA の 2 本のピークが得られた。標識 siRNA のピークを LC で分離し、ESI-TOF-MS を用いて分析した。その結果、F 標識 siRNA に該当する多価イオンのピークが得られた (図 1) 。同様の条件にてポジトロン標識 siRNA を分析し、^{18}F 標識 siRNA の分取に成功した。この ^{18}F 標識 siRNA が合成中に分解を受けていないことを電気泳動にて確認し、インビボ解析への応用が可能であることを明らかにした。

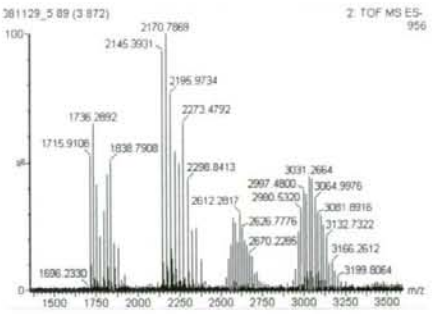

図 1　F 標識 siRNA の LC/ESI-TOF-MS データ

(2) siRNA 体内動態の PET 解析

ポジトロン標識 siRNA 単体およびリポソームに搭載したポジトロン標識 siRNA をマウスに尾静脈内投与し、それぞれの体内動態を比較した。siRNA 単体では体内で速やかに分解され、腎臓を経て膀胱排泄される様子が観察された。一方で、カチオニックリポソームに搭載した siRNA は初回通過臓器である肺に集積する様子が観察された (図 2)。リアルタイムイメージング後に各臓器における放射活性を測定した結果、^{18}F の分布がイメージングデータと一致していることが確認された。

図 2　^{18}F 標識 siRNA の PET イメージングデータ

(3) 類似技術との比較検討

主薬である siRNA とベクターであるリポソームの体内動態が一致しているか否かを評価していくうえで、実際にリポソームの動態解析方法について検討した。申請者らが開発したポジトロン標識プローブを用いてリポソームを標識し、PET 解析によってその体内動態を明らかにした。

また、Alexa750 標識 siRNA をマウスに尾静脈内投与し、蛍光インビボイメージングシステムを用いて解析した。その結果、PET とは測定原理がまったく異なるゆえ、蛍光法では体表面のシグナルが強調された。蛍光法では体表面からの深度の影響が大きく、非侵襲的なリアルタイムイメージングと解剖後の *ex vivo* データに差が生じた。その一方で、蛍光インビボイメージングシステムが PET 解析データの検証に有用な手段であることが明らかとなった。

D. 考察

本年度は、ポジトロン標識 siRNA の設計と合成に関して計画を遂行し、実際に PET 解析を開始するまでに至った。まず、siRNA 検出法として LC/ESI-TOF-MS の分析条件を確立した。同様にポジトロン標識 siRNA を分離可能な分析条件を確立し、PET 解析の基礎的検討に移行するに至った。一方で、蛍光インビボイメージングによる siRNA 体内動態解析を実施し、PET 技術の優位性を示した。また、PET を用いてポジトロン標識リポソームの体内動態を解析し、基礎的データを取得した。以上のように、siRNA 体内動態の PET 解析技術の確立に向け、多くの基礎的なデータが得られた。

本課題研究における検討を継続し、siRNA 体内動態の PET 解析技術の確立に至れば、治療効果を予測するうえでも DDS 製剤の設計に情報をフィードバックするうえでも極めて貴重な解析データが得られるようになる。したがって、siRNA やそのキャリアなどにおいて有望なシーズを保有している企業ならびに公的機関に対して魅力的な動態解析技術を提供できるようになる。医薬品候補の siRNA の体内動態に関して有益な情報が得られることにより、RNA 創薬の開発効率を高め、創薬の加速化に結び付くと考えられる。さらに PET 技術は、ヒトマイクロドーズ試験への応用に発展する可能性を有しており、これが実現すればさらなる開発効率の向上が期待できる。以上のように、本研究の目標が達成されることにより、国民を悩ます疾病の克服を目指した医薬品開発に大きな波及効果を生むことができる可能性がある。

E. 結論

初年度の研究事業計画はほぼ予定通りに遂行しており、siRNA 体内動態の PET 解析技術の確立に向けて、着実に研究成果が得られた。2 年目となる次年度には、siRNA 体内動態の PET 解析技術の確立および蛍光インビボイメージング法との比較検証、ポジトロン標識 siRNA を搭載した各種ベクターの動態解析を重点的に取り組む計画である。本研究事業の目標を計画通りに達成し、開発する技術が RNA 創薬の加速化に繋がることを期待している。

F. 研究発表

1. 論文発表

1) Urakami, T., Sakai, K., Asai, T., Fukumoto, D., Tsukada, H., Oku, N.: Evaluation of O-[(18)F] fluoromethyl-d-tyrosine as a radiotracer for tumor imaging with positron emission tomography. *Nucl. Med. Biol.*, **36**, 295-303. (2009)

2) Takahama, H., Minamino, T., Asanuma, H., Fujita, M., Asai, T., Wakeno, M., Sasaki, H., Kikuchi, H., Hashimoto, K., Oku, N., Asakura, M., Kim, J., Takashima, S., Komamura, K., Sugimachi, M., Mochizuki, N., Kitakaze, M.: Prolonged targeting of ischemic/reperfused

myocardium by liposomal adenosine augments cardioprotection in rats. *J. Am. Coll. Cardiol.*, **53**, 709-717. (2009)

3) Urakami, T., Kawaguchi, A.T., Akai, S., Hatanaka, K., Koide, H., Shimizu, K., Asai, T., Fukumoto, D., Harada, N., Tsukada, H., Oku, N.: In vivo distribution of liposome-encapsulated hemoglobin determined by positron emission tomography. *Artif. Organs*, **33**, 164-168. (2009)

4) Koide, H., Asai, T., Hatanaka, K., Urakami, T., Ishii, T., Kenjo, E., Nishihara, M., Yokoyama, M., Ishida, T., Kiwada, H., Oku, N.: Particle size-dependent triggering of accelerated blood clearance phenomenon. *Int. J. Pharm.*, **362**, 197-200. (2008)

5) Katanasaka, Y., Ida, T., Asai, T., Maeda, N., Oku, N.: Effective delivery of an angiogenesis inhibitor by neovessel-targeted liposomes. *Int. J. Pharm.* **360**, 219-224. (2008)

6) Katanasaka, Y., Ida, T., Asai, T., Shimizu, K., Koizumi, F., Maeda, N., Baba, K., Oku, N.: Antiangiogenic cancer therapy using tumor vasculature-targeted liposomes encapsulating 3-(3,5-dimethyl-1H-pyrrol-2-ylmethylene)-1,3-dihydro-indol-2-one, SU5416. *Cancer Lett.*, **270**, 260-268. (2008)

2. 学会発表

・招待講演

1) Asai, T., Oku, N.: Angiogenic vessel-targeted liposomes for *in vivo* delivery of siRNA. Japan Society of Gene Therapy The 14th Annual Meeting 2008 (Sapporo, Japan) Educational Seminar V-1. 2008 年 6 月 14 日

2) Asai, T, Oku, N.: Angiogenic vessel-targeted liposomal DDS for cancer treatment. 11th Liposome Research Days Conference (Yokohama, Japan) Program book, p.63. 2008 年 7 月 20 日

・一般講演

1) 庭田佳代子、浅井知浩、出羽毅久、南後 守、奥 直人：ポリカチオンリポソームを用いた遺伝子導入におけるポリアミン構造が導入効率に及ぼす効果．日本薬剤学会第 23 回年会（札幌）、講演要旨集、p.132. 2008 年 5 月 20 日

2) Matsushita, S., Asai, T., Suzuki, Y., Ishida, T., Maeda, N., Dewa, T., Kiwada, H., Nango, M., Oku, N.: Development of angiogenic vessel-targeted polycation liposomes for delivering small interfering RNA. 35th Annual Meeting & Exposition of the Controlled Release Society (New York, USA) Program book, p.88. 2008 年 7 月 16 日

3) Niwata, K., Asai, T., Dewa, T., Nango, M., Oku, N.: Development of novel polycation liposomes for gene transfer system. 35th Annual Meeting & Exposition of the Controlled Release Society (New York, USA) Program book, p.88. 2008 年 7 月 16 日

4) Oku, N., Urakami, T., Asai, T., Akai, S., Tsukada, H., Kawaguchi, A.: Microdosing test for liposomal drugs. 11th Liposome Research Days Conference (Yokohama, Japan) Program book, p.73. 2008 年 7 月 20 日

5) Katayama, Y., Urakami, T., Akai, S., Yokoyama, M., Kawaguchi, A., Tsukada, H., Asai, T., Oku N.: A novel labeling method for PET imaging on the development of liposomal DDS drugs. 11th Liposome Research Days Conference (Yokohama, Japan) Program book, p.128. 2008 年 7 月 20 日

6) Kenjo, E., Tsuruta, A., Hatanaka, K., Asai, T., Dewa, T., Nango, M., Oku, N.: Development of liposomal siRNA targeting tumor angiogenic vessels. 11th Liposome Research Days

Conference (Yokohama, Japan) Program book, p.257. 2008 年 7 月 21 日

7) Matsushita, S., Asai, T., Suzuki, Y., Tatsuhiro Ishida, Noriyuki Maeda, Takehisa Dewa, Hiroshi Kiwada, Mamoru Nango, Naoto Oku: Antiangiogenic effect by Argonaute2 knockdown used polycation liposome. 11th Liposome Research Days Conference (Yokohama, Japan) Program book, p.171. 2008 年 7 月 22 日

8) 片山百合恵、浦上武雄、山下美菜、赤井周司、川口 章、塚田秀夫、浅井知浩、奥 直人：病態モデルラットにおけるリポソーム製剤の PET 動態解析. 第 17 回 DDS カンファランス（静岡）、講演要旨集、p.14. 2008 年 9 月 20 日

G. 知的財産権の出願・登録状況

なし

研究成果の刊行に関する一覧表

雑誌

発表者氏名	論文タイトル名	発表誌名	巻号	ページ	出版年
Urakami, T., Sakai, K., Asai, T., Fukumoto, D., Tsukada, H., Oku, N.	Evaluation of O-[(18)F]fluoromethyl-d-tyrosine as a radiotracer for tumor imaging with positron emission tomography.	*Nucl Med Biol.*	**36**	295-303	2009
Takahama, H., Minamino, T., Asanuma, H., Fujita, M., Asai, T., Wakeno, M., Sasaki, H., Kikuchi, H., Hashimoto, K., Oku, N., Asakura, M., Kim, J., Takashima, S., Komamura, K., Sugimachi, M., Mochizuki, N., Kitakaze, M..	Prolonged targeting of ischemic/reperfused myocardium by liposomal adenosine augments cardioprotection in rats.	*J. Am. Coll. Cardiol.*	**53**	709-717	2009
Urakami, T., Kawaguchi, A.T., Akai, S., Hatanaka, K., Koide, H., Shimizu, K., Asai, T., Fukumoto, D., Harada, N., Tsukada, H., Oku, N.	In vivo distribution of liposome-encapsulated hemoglobin determined by positron emission tomography.	*Artif. Organs*	**33**	164-168	2009
Koide, H., Asai, T., Hatanaka, K., Urakami, T., Ishii, T., Kenjo, E., Nishihara, M., Yokoyama, M., Ishida, T., Kiwada, H., Oku, N.	Particle size-dependent triggering of accelerated blood clearance phenomenon.	*Int. J. Pharm.*	**362**	197-200	2008
Katanasaka, Y., Ida, T., Asai, T., Maeda, N., Oku, N.	Effective delivery of an angiogenesis inhibitor by neovessel-targeted liposomes.	*Int. J. Pharm.*	**360**	219-224	2008

Katanasaka, Y., Ida, T., Asai, T., Shimizu, K., Koizumi, F., Maeda, N., Baba, K., Oku, N.	Antiangiogenic cancer therapy using tumor vasculature-targeted liposomes encapsulating 3-(3, 5-dimethyl-1H-pyrrol-2-ylmethylene)-1,3-dihydro-indol-2-one, SU5416.	*Cancer Lett.*	**270**	260-268	2008

Available online at www.sciencedirect.com
ScienceDirect
Nuclear Medicine and Biology 36 (2009) 295–303
NUCLEAR MEDICINE — AND — BIOLOGY
www.elsevier.com/locate/nucmedbio

Evaluation of *O*-[^{18}F]fluoromethyl-D-tyrosine as a radiotracer for tumor imaging with positron emission tomography☆

Takeo Urakami[a], Koichi Sakai[b], Tomohiro Asai[a], Dai Fukumoto[b], Hideo Tsukada[b], Naoto Oku[a,*]

[a]*Department of Medical Biochemistry and Global COE, University of Shizuoka Graduate School of Pharmaceutical Sciences, Yada, Suruga-ku, Shizuoka 422-8526, Japan*

[b]*PET Center, Central Research Laboratory, Hamamatsu Photonics K.K., Hamamatsu, Shizuoka 434-8601, Japan*

Received 14 April 2008; received in revised form 3 December 2008; accepted 24 December 2008

Abstract

O-[^{18}F]Fluoromethyl-D-tyrosine (D-[^{18}F]FMT) has been reported as a potential tumor-detecting agent for positron emission tomography (PET). However, the reason why D-[^{18}F]FMT is better than L-[^{18}F]FMT is unclear. To clarify this point, we examined the mechanism of their transport and their suitability for tumor detection. The stereo-selective uptake and release of enantiomerically pure D- and L-[^{18}F]FMT by rat C6 glioma cells and human cervix adenocarcinoma HeLa cells were examined. The results of a competitive inhibition study using various amino acids and a selective inhibitor for transport system L suggested that D-[^{18}F]FMT, as well as L-[^{18}F]FMT, was transported via system L, the large neutral amino acid transporter, possibly via LAT1. The in vivo distribution of both [^{18}F]FMT and [^{18}F]FDG in tumor-bearing mice and rats was imaged with a high-resolution small-animal PET system. In vivo PET imaging of D-[^{18}F]FMT in mouse xenograft and rat allograft tumor models showed high contrast with a low background, especially in the abdominal and brain region. The results of our in vitro and in vivo studies indicate that L-[^{18}F]FMT and D-[^{18}F]FMT are specifically taken up by tumor cells via system L. D-[^{18}F]FMT, however, provides a better tumor-to-background contrast with a tumor/background (contralateral region) ratio of 2.741 vs. 1.878 with the L-isomer, whose difference appears to be caused by a difference in the influence of extracellular amino acids on the uptake and excretion of these two isomers in various organs. Therefore, D-[^{18}F]FMT would be a more powerful tool as a tumor-detecting agent for PET, especially for the imaging of a brain cancer and an abdominal cancer.

Keywords: *O*-[^{18}F]Fluoromethyl tyrosine; D-isomer; Positron emission tomography (PET); System L transporter; Tumor imaging

1. Introduction

[^{18}F]FDG is the most widely used tracer for tumor detection with PET imaging. However, several limitations with [^{18}F]FDG have been reported, such as a high uptake in normal brain and heart and in inflammatory tissues [1]. In contrast, the accumulation of positron emitter-labeled amino acids was assumed to reflect enhanced amino acid transport, metabolism and protein synthesis. Therefore, these amino acid tracers have been used for detecting tumors especially those in the brain.

Positron emitter-labeled amino acids and their derivatives, such as 1-[^{11}C]methionine [2], methyl-[^{11}C]methionine [2,3], 1-[^{11}C]tyrosine [4], 1-[^{11}C]leucine [5], 1-[^{11}C]phenylalanine [6], 4-[^{18}F]fluoro-phenylalanine [7] and 2-[^{18}F]fluoro-L-tyrosine [8], have been proposed as PET imaging agents. Among these positron emitter-labeled amino acids, [^{11}C]methionine is widely used for tumor imaging with PET. Recently, several amino acid analogs, namely, *O*-[^{11}C]methyl-L-tyrosine [9], *O*-[^{18}F]fluoromethyl-L-tyrosine (L-[^{18}F]FMT) [9], *O*-[^{18}F]fluoroethyl-L-tyrosine [10,11], *O*-[^{18}F]fluoropropyl-L-tyrosine [12,13], [^{11}C]ethyonine [14] and [^{11}C]propionine [14], were synthesized and evaluated as PET imaging agents. These amino acid

☆ This study was supported by a grant from the Central Shizuoka Cooperation of Innovative Technology and Advanced Research in Evolution Area (City Area) supported by the Ministry of Education, Culture, Sports, Science and Technology of Japan (MEXT); and also by the Research and Development of Technology for Measuring Vital Function Merged with Optical Technology, MEXT; and by the Research and Development Project Aimed at Economic Revitalization, MEXT.

* Corresponding author. Tel.: +81 54 264 5701; fax: +81 54 264 5705.
E-mail address: oku@u-shizuoka-ken.ac.jp (N. Oku).

0969-8051/$ – see front matter © 2009 Published by Elsevier Inc.
doi:10.1016/j.nucmedbio.2008.12.012

analogues showed relatively low accumulation in normal peripheral tissue (low tissue-to-blood ratio), rapid blood clearance and a rather high amount of label remaining in tumor tissues (high tumor-to-blood ratio).

In contrast to L-isomers of amino acids, D-isomers are considered to behave as unnatural amino acids, like the amino acid analogs mentioned above. In previous reports in the 1980s, in vivo and in vitro experiments using ^{14}C-labeled D-amino acids revealed that the accumulation of D-isomers was higher than that of L-isomers in tumor cells [15,16]. At that time, the potential of D-isomers of amino acids as nuclear imaging agents was mentioned [15–17]. However, the precise mechanism responsible for the higher accumulation of the D-isomers has remained unclear. Recently, the biological functions of D-isomers in the central nervous system [18], developmental biology [19] and some pathological conditions [20,21] were reported, although the precise behavior of D-isomers still remains to be clarified [22].

Amino acid transport across the plasma membrane is mediated via amino acid transporters located on the membrane. Among the amino acid transport systems, system L, a Na^+-independent neutral amino acid transporter system, is the major route for providing cells with large neutral amino acids including branched or aromatic amino acids [23]. Recently, system L amino acid transporters 1 and 2 (LAT1 and LAT2) were isolated, and their characteristics were evaluated [24–26]. LAT1 was shown to be strongly expressed in malignant tumors [27,28] and also expressed in some normal organs such as brain, spleen, placenta and testis [29]. In contrast, the distribution of LAT2 mRNA is ubiquitous [30,31]. We previously reported that the D-isomer of *O*-[^{18}F]fluoromethyl-L-tyrosine (D-[^{18}F]FMT) was highly accumulated in tumor tissue [32,33], although the accumulation of D-[^{18}F]FMT in normal tissues, e.g., brain, kidney and pancreas, was low as was the whole-body background. However, the molecular mechanism of D-[^{18}F]FMT uptake in tumor tissue was not addressed at that time. Since the presence of amino acids in plasma would affect the uptake of this tracer into tissues, the concentrations of amino acids in plasma, in normal and tumor tissues, and in the microenvironment of tumor cells must be considered [34].

In this study, the characteristics and utility of the D-isomer of an artificial amino acid labeled with ^{18}F positron emitter were evaluated; and the behavior of L-[^{18}F]FMT and D-[^{18}F]FMT both in vitro and in vivo was examined.

2. Materials and methods

2.1. Materials

L-Alanine, L-glycine, L-phenylalanine, L-serine, D-leucine and L-leucine were purchased from Wako Pure Chemical Co. Ltd. (Osaka, Japan). 2-Aminobicyclo-(2,2,1)-heptane-2-carboxylic acid (BCH) was obtained from Sigma-Aldrich Japan (Tokyo, Japan). All other reagents were of analytical grade.

2.2. Synthesis of labeled compound

Positron-emitting ^{18}F was produced by $^{18}O(p,n)^{18}F$ nuclear reaction using the cyclotron (HM-18; Sumitomo Heavy Industry, Japan) at Hamamatsu Photonics PET Center. L- and D-Isomers of [^{18}F]FMT were synthesized by reacting [^{18}F]fluoro-methyl bromide with the corresponding L- and D-tyrosine according to a previous report [32,33]. Enantiomeric purity was analyzed on a CHIOBIOTIC T column (4.6×250 mm; Tokyo Kasei Kogyo). The elution solution was ethanol/water (1:1), and the flow rate was 1 ml/min. The production of [^{18}F]FDG was performed according to the method reported previously [35]. Specific activities of D-[^{18}F]FMT, L-[^{18}F]FMT and [^{18}F]FDG were 115±10, 126±12 and 144±21 GBq/μmol, respectively; and radiochemical purities were 99.6±0.4%, 99.8±0.3% and 100.0±0.0%, respectively.

2.3. Cell culture

C6 glioma cells (ATCC, Rockville, MD, USA) and HeLa cells (RIKEN, Tsukuba, Japan) were grown in Dulbecco's Modified Eagle's Medium (DMEM, Wako) supplemented with 10% fetal bovine serum (Japan Bioserum, Hiroshima, Japan) and appropriate concentrations of antibiotics (100 U/ml penicillin and 100 μg/ml streptomycin). The cells were maintained in plastic culture flasks at 37°C in a humidified atmosphere containing 5% CO_2 and kept as monolayers.

2.4. Measurement of uptake by cells in culture

Rat C6 glioma cells and HeLa cells were plated in 24-well culture plates (Corning Japan, Tokyo, Japan) at a density of 2×10^5 cells per well and cultured for 24 h. After the growth medium had been removed, the cells were washed twice with Hank's balanced salt solution (HBSS; 136.6 mM NaCl, 5.4 mM KCl, 4.2 mM $NaHCO_3$, 1 mM $CaCl_2$, 0.5 mM $MgCl_2$, 0.44 mM KH_2PO_4 and 0.41 mM $MgSO_4$) and kept in HBSS for 30 min at 37°C to deplete any residual nutrients from the growth medium. Then the HBSS was discarded, and the uptake assay was started by adding a trace amount of D- or L-isomer of [^{18}F]FMT/HBSS (1–3 MBq/ml) to the cultures. After incubation for the selected time period (2, 5, 10, 30 and 60 min), the uptake of labeled compounds was terminated by removing the medium. After the cells had been washed twice with 1 ml of ice-chilled Dulbecco's phosphate-buffered saline (PBS), the cells were lysed in 400 μl of cell lysis solution (0.1 M NaOH, 2% Triton X-100). The radioactivity in the cell lysates was measured by a γ-counter (Aloka ARC-2000). More than three independent experiments, each done in triplicate, were performed.

2.5. Tracer release from cultured cells

Experiments were performed using 24-well culture plates. HeLa cells (2×10^5 cells/well) were incubated with D- or L-isomer of [^{18}F]FMT (1-3 MBq/ml) in HBSS for 30 min at 37°C. Then, the cells were washed three times with HBSS, and all supernatants were discarded. Release experiments were started by the addition of 1 ml HBSS. The supernatant

was collected at each time point from each well, and cells in the well were washed twice with ice-chilled PBS very quickly. Then the cells were lysed with 400 μl of cell lysis solution (0.1 M NaOH, 2% Triton X-100), and the radioactivity in the cell lysates was measured by a γ-counter. More than three independent experiments, each done in triplicate, were performed.

2.6. Reverse transcriptase–polymerase chain reaction

Total RNAs were isolated from C6 glioma and HeLa cells by using an RNA purification kit (QIAshredder and RNeasy kit, QIAGEN KK, Tokyo, JAPAN) in accordance with the manufacturer's instructions. Then, the first-strand cDNAs were prepared with a Superscript First-strand Synthesis system (Invitrogen Japan KK, Tokyo, Japan) and oligo(dT) primer, and used as a template for polymerase chain reaction (PCR) amplification. The PCR amplification was performed with Ex Taq (Takara Bio, Inc., Ohtu, Japan) according to the following protocol [27]: 94°C for 5 min, followed by 25 cycles of 94°C for 30 s, 60°C for 30 s and 72°C for 1 min and a final extension step of 72°C for 10 min. The following primer pairs were used for PCR amplification: 5′-CAATGGTGTGGCCATCATG-3′ and 5′-GATGCATCCCCTTGTCCTAT-3′ for rat LAT1, 5′-TCATTGGCTCCGGAATCTTC-3′ and 5′-ATGCA TTCTTTGGCTCCAGC-3′ for rat LAT2, 5′-TCACAGGCT-TATCCAAGGAG-3′ and 5′-TACAATGTCAGCCTGAG-GAG-3′ for rat 4F2hc, 5′-TTCATCGCA- GTACATCG-TGG-3′ and 5′-CCCAGGTGATAGTTCCCGAA-3′ for human LAT1, 5′-AGCCCTGAAGAAAGAGATCG-3′ and 5′-TGCATATCTGTACAATCCCC-3′ for human LAT2, 5′-TCGATTACCTGAGCTCTCTG-3′ and 5′-GGGATTTTG-TATGCTCCCCA-3′ for human 4F2hc and 5′-TGACGGGGTCACCCACACTGTGCCCATCTA-3′ and 5′-CTAGAAGCATTTGCGGTGGACGATGGAGGG-3′ for human and rat β-actin.

2.7. Animals

All animals were maintained and handled in accordance with the recommendations of the National Institutes of Health and the Animal Facility Guidelines of the University of Shizuoka.

The mice bearing tumors were prepared as reported previously [32]. Briefly, female BALB/cA Jcl-nu mice (7 weeks old) were inoculated subcutaneously with 5×10^6 HeLa cells, maintained for 2 weeks after the transplantation and used for experiments at 9 weeks of age.

Male Fischer rats (9 weeks old) were obtained from Japan SLC, Inc. The rat C6 brain tumor model was prepared as reported elsewhere with a minor modification [36]. Rats were anesthetized with chloral hydrate and individually placed in a stereotaxic apparatus. C6 glioma cells (2×10^5 cells/10 μl of DMEM containing 1% gelatin) were injected at a rate of 1.0 μl/min into the left hippocampus of the rat (−4.7 mm posterior to bregma, −3.9 mm lateral to the midline suture and −6.2 mm from the dura) via a 28-gauge stainless tube. Eleven days after tumor implantation, the rats were used for PET studies.

2.8. Whole-body imaging of tumor-bearing mice and rats

The distribution pattern of each radiolabeled compound in the rats was determined with a small-animal PET system (Clairvivo PET, Shimadzu, Kyoto, Japan). Animals were anesthetized by an intraperitoneal injection of chloral hydrate at 400 mg/kg, followed by continuous infusion of the anesthetic at 100 mg/kg per hour through a cannula placed into a tail vein. Anesthetized rats were fixed on an animal holder. Each ^{18}F-radiolabeled compound at a dose of 7 MBq was injected intravenously into each rat via a tail vein. The data were obtained with a list mode data acquisition every 1 s for 60 min. Reconstruction was made by 3D-DRAMA (two iterations, γ=0.1) with resolution modeling. After the PET analysis, the rat brains were excised and sliced into eight coronal slices of 2-mm thickness (four slices anterior to and four slices posterior to the optical chiasm) with a brain slicer (Muromachi Kikai, Co. Ltd, Tokyo, Japan). The distribution of [^{18}F]FMT or [^{18}F]FDG in each brain slice was determined by autoradiography after exposure to an imaging plate for approximately 1 h. The autoradiograms of the brain slices were obtained by using a Bio-imaging analyzer BAS1500 and analyzed by Image Gauge V3.45 (Fuji Photo Film, Co. Ltd, Tokyo, Japan).

3. Results

3.1. Uptake and release of [^{18}F]FMT in vitro

The enantiomeric purity of each isomer was determined by the enantiomeric analytic HPLC as reported previously [33]. The results showed the enantiomeric purity of each isomer to be more than 98%.

At first, we examined the transport of the D- and L-isomers of [^{18}F]FMT in rat C6 glioma cells and HeLa cells. The uptake of D- and L-isomers of [^{18}F]FMT into these cells was measured at selected time points up to 30 min. As a result, the uptake rate of the L-isomer was significantly higher than that of the D-isomer in both C6 glioma and HeLa cells (Fig. 1). The uptake was not saturated at least up to 60 min (data not shown).

Then, the release of the D- and L-isomers from HeLa cells in the presence or absence of 100 μM L-leucine was examined. As shown in Fig. 2A, the release of the D-isomer under the amino acid-free condition in HBSS was slower than that of L-isomer. On the other hand, the release rate of both L-[^{18}F]FMT and D-[^{18}F]FMT was accelerated in the presence of L-leucine (Fig. 2B). These uptake and release experimental results on [^{18}F]FMT indicate that the amino acid transport activity of the D-isomer was lower than that of the L-isomer in both C6 glioma and HeLa cells in vitro. Then, we further examined the selectivity of the transporter by performing inhibition experiments in C6 glioma cells. The uptake of D- and L-isomers of [^{18}F]FMT was strongly inhibited in the presence of 1 mM L-isomers of methionine, phenylalanine and tyrosine (Fig. 3A). The uptake was also

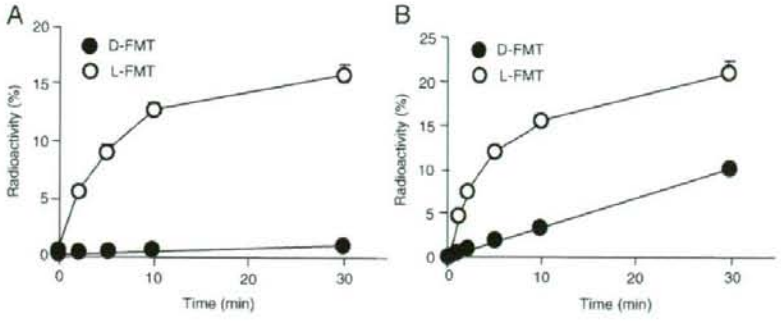

Fig. 1. Time-dependent uptake of D- and L-isomers of [^{18}F]FMT by C6 glioma and HeLa cells. The C6 glioma (A) and HeLa (B) cells were incubated for 1, 2, 5, 10 or 30 min in uptake solution containing 1–3 MBq of D- or L-isomers of [^{18}F]FMT. The relative radioactivity (as a percentage of the total dose) at each point is indicated as the mean±S.D. More than three independent experiments, each done in triplicate, were performed.

inhibited by BCH, a selective inhibitor of the system L amino acid transporter. However, the uptake was not inhibited by L-glycine. These inhibition patterns in the presence of amino acids for uptake of D- and L-isomers of [^{18}F]FMT were essentially the same, suggesting that both D- and L-isomers of [^{18}F]FMT were taken up by the same transporter, namely, the system L amino acid transporter.

Since the activity of the system L amino acid transporter is reported to be independent of extracellular sodium ions [24,25], we next examined the sodium ion dependency of the D- and L-[^{18}F]FMT transport. A sodium ion-free condition was obtained by substitution of sodium chloride with choline chloride, as reported previously [25]. Fig. 3B shows the sodium ion-independent uptake of both D- and L-isomers. These results support the idea that both D- and L- isomers of [^{18}F]FMT are transported by system L amino acid transporters.

Next, the effect of the competitive inhibition of the system L amino acid transporter on the uptake of D- or L-isomer of [^{18}F]FMT was examined. D-[^{18}F]FMT or L-[^{18}F]FMT was loaded into HeLa cells in the presence of the various concentrations of BCH, a selective inhibitor of system L (Fig. 4A). The uptake of both D- and L-isomers of [^{18}F]FMT was inhibited by BCH in a dose- dependent manner. Furthermore, the inhibitory effect of various concentrations of natural amino acids, i.e., D- and L-leucine, on isomer uptake was examined. Both D- and L-leucine inhibited the uptake of [^{18}F]FMT; however, L-[^{18}F]FMT uptake was decreased more at a low concentration of the extracellular amino acids (Fig. 4B and C) than the D-isomer. These results suggest that the transport of L-[^{18}F]FMT was more affected in the presence of either L-leucine or D-leucine than that of the D-isomer in vitro and that this might also be the case in vivo.

System L amino acid transporter proteins LAT1 and LAT2 were isolated previously. LAT1 and LAT2 require an additional single-membrane-spanning protein heavy chain of the 4F2 antigen (4F2hc) for their functional expression in the plasma membrane. LAT1 and 4F2hc or LAT2 and 4F2hc form a heterodimeric complex via a disulfide bond. So we examined the mRNA expression of the system L amino acid transporters in C6 glioma and HeLa cells. In the reverse

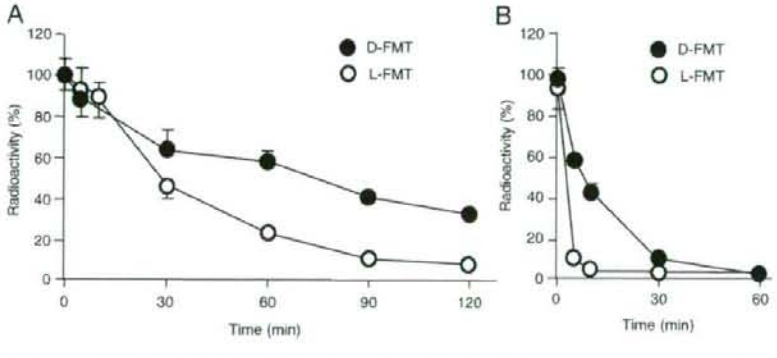

Fig. 2. Release of D- and L-isomers of [^{18}F]FMT preloaded in HeLa cells. The release of preloaded [^{18}F]FMT from HeLa cells was examined. The cells preloaded with D- or L-isomers of [^{18}F]FMT were incubated in the absence (A) or presence (B) of 100 μM L-leucine. The relative radioactivities that remained in the cells were determined to obtain the release rate of [^{18}F]FMT. Each point indicates the mean±S.D. More than three independent experiments, each carried out in triplicate, were performed.

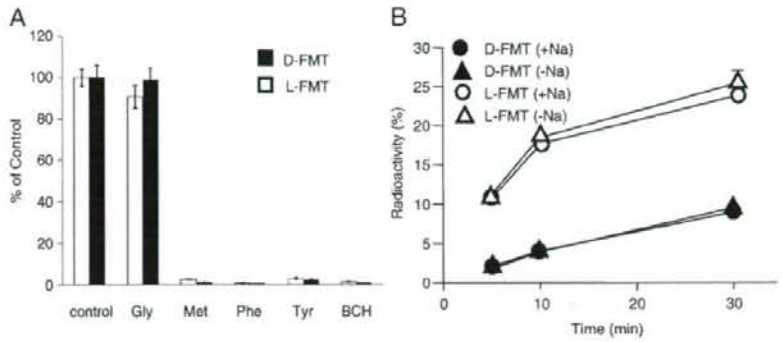

Fig. 3. Uptake of D- and L-isomers of [^{18}F]FMT by C6 glioma cells in the presence of amino acids, inhibitors and Na^+ ions. (A) C6 glioma cells were incubated with D- or L-isomer of [^{18}F]FMT in the uptake solution containing L-glycine, L-methionine, L-phenylalanine, L-tyrosine or BCH (100 μM for each). The relative radioactivity in the cells was determined. (B) C6 glioma cells were incubated with D- or L-isomer of [^{18}F]FMT in the uptake solution in the presence (circles) or absence (triangles) of Na^+ ions. The relative radioactivity of cells was determined. Data are presented as the relative mean uptake±S.D.

transcriptase–PCR (RT-PCR) analysis, the PCR products for LAT1 and their associating protein 4F2hc, but not the LAT2 product, were detected when RNA from the rat C6 glioma and HeLa cell cultures was used (Fig. 5).

3.2. Tumor PET imaging with [^{18}F]FMT

Noninvasive real-time imaging with a small-animal PET provides distribution data consistent with those obtained from tissue dissection assays. Mice xenografted with HeLa cells were prepared and examined by PET. Data were acquired from mice administered D-[^{18}F]FMT, L-[^{18}F]FMT or [^{18}F]FDG (Fig. 6). The mouse injected with D-[^{18}F]FMT showed the clearest difference in tracer intensity between the tumor (right leg) and the normal tissue (left leg) compared with the mice given the other tracers. The accumulation of D-[^{18}F]FMT in the tumor tissue was not different from that of L-[^{18}F]FMT. The standard uptake value (SUV) of the former was 1.336; and that of the latter, 1.642. However,

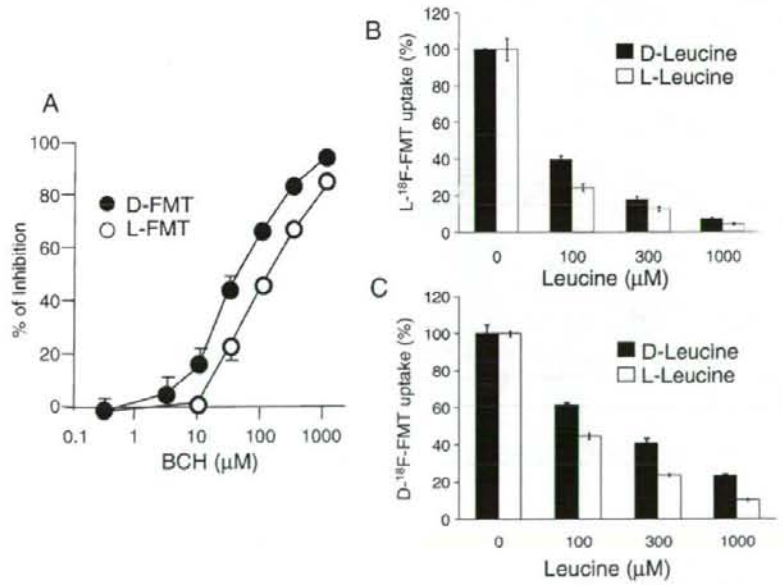

Fig. 4. BCH- and L- or D-leucine-mediated inhibition of D- or L-[^{18}F]FMT uptake by HeLa cells. The uptake of D- (open circle) or L-isomer (closed circle) of [^{18}F]FMT was measured for 5 min in the presence of various concentrations of BCH (A). The stereo-selective inhibitory effect of leucine on the uptake of L-[^{18}F]FMT (B) and D-[^{18}F]FMT (C) into HeLa cells was examined in the presence of 0, 100, 300 and 1000 μM L- or D-leucine. The graph shows the % radioactivity of the control (without leucine). Bars indicate the mean±S.D.

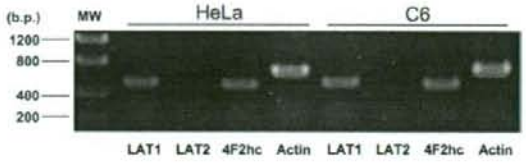

Fig. 5. RT-PCR detection of LAT1, LAT2 and 4F2hc mRNAs in HeLa and C6 cells. First-strand cDNAs prepared from cultured C6 glioma and HeLa cells were used as templates for PCR amplification. The PCR products were subjected to agarose gel electrophoresis and visualized with ethidium bromide.

there was far less radioactivity in the normal tissue in the case of the image obtained with the D-isomer of [^{18}F]FMT: SUVs for D-[^{18}F]FMT and L-[^{18}F]FMT were 0.488 and 0.874, respectively.

Finally, the in vivo tumor imaging in the brain tumor model was examined. Data were displayed as the image of

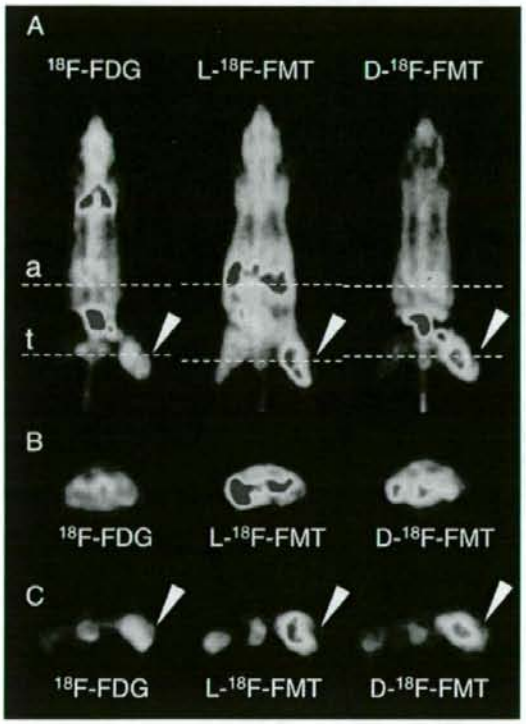

Fig. 6. Small-animal PET images of [^{18}F]FDG, L-[^{18}F]FMT and D-[^{18}F]FMT in tumor-bearing mice. Mice were inoculated with HeLa cells, and radiolabeled compounds were injected intravenously for the PET imaging. Coronal plane images (A), axial plane images of the abdominal region (B) and axial plane images of tumor implanted region (C) after injection of [^{18}F] FDG, L-[^{18}F]FMT or D-[^{18}F]FMT are shown. The broken lines "a" and "t" indicate the position of the axial plane image of the abdominal region (B) and the tumor region (C), respectively. The arrowhead points to the tumor. The typical images from multiple independent experiments (n>3) are shown.

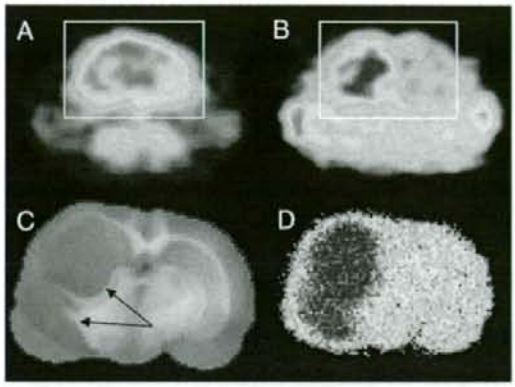

Fig. 7. Small-animal PET images of D-[^{18}F]FMT and [^{18}F]FDG in a brain tumor-bearing rat. PET imaging of [^{18}F]FDG (A) and D-[^{18}F]FMT (B) was performed in the same rat bearing a C6 glioma brain tumor. The brain area in the PET image is indicated by the square. After the PET study with D-[^{18}F] FMT, brain slices were prepared to confirm the location of the tumor (arrows, C) and to detect the radioactivity of D-[^{18}F]FMT in the brain by autoradiography (D). Note that images in (C) and (D) are expanded beyond the square region (brain). Five separate experiments were performed, and similar results were obtained. Data typical of one of them are shown here.

the D-isomer of [^{18}F]FMT in comparison with that of [^{18}F] FDG in the rat C6 glioma orthotopic brain tumor model, as shown in Fig. 7. In this model of brain tumor, [^{18}F]FDG could not detect the tumor specifically due to the high background in the normal brain tissue (Fig. 7A). In contrast, D-[^{18}F]FMT showed a lower accumulation in the normal region of the brain (Fig. 7B), and thus the tumor region in the brain was imaged. (Comment in Fig. 7C and D).

4. Discussion

In the present study, we investigated the properties of ^{18}F-labeled D- and L-isomers of artificial amino acid FMT in relation to their transport activity in cultured C6 glioma and HeLa cells. In addition, the specificity of amino acid transporters engaged in the transport of D- and L-isomers of [^{18}F]FMT was examined.

Concerning ^{18}F-PET studies, positron emitter-labeled diagnostic drugs possess very high specific radioactivity: specific activities of D-[^{18}F]FMT, L-[^{18}F]FMT and [^{18}F]FDG in the present study were 115±10, 126±12 and 144±21 GBq/μmol, respectively. Therefore, the experiment was performed by using amino acids at the tracer level concentration. The uptake study on the D- and L- isomers of [^{18}F]FMT in C6 glioma and HeLa cells in HBSS suggested that the incorporation was mediated by a stereo-selective amino acid transporter, since the L-isomer was incorporated much faster than the D-isomer (Fig. 1).

The release of D- and L-isomers of [^{18}F]FMT was examined by use of HeLa cells preloaded with each isomer

of [^{18}F]FMT. The release of D-[^{18}F]FMT from the cells was slower than that of L-isomer (Fig. 2A). This result is consistent with the uptake data. Since intra/extracellular amino acid exchange was reported as a feature of the system L amino acid transport system [25], the presence of extracellular amino acid would enhance the release of intracellular [^{18}F]FMT in system L. In fact, the release of both D- and L-isomers of [^{18}F]FMT was up-regulated by extracellular 100 μM L-leucine, a typical substrate of system L (Fig. 2B). The physiological concentration of leucine in human plasma is approx. 100 μM, as reported previously [34,37]. Considering the situation of tumor cells in the living body, there would be plenty of extracellular amino acids in the plasma; and they would have an effect on both the uptake and release of amino acid-related PET tracers.

To clarify the involvement of the transport system in [^{18}F]FMT uptake, we examined the inhibition of uptake of the D- or L-isomer of [^{18}F]FMT by the L-isomer of various amino acids and by a system L selective inhibitor, BCH, in C6 glioma cells. BCH is an amino acid-related compound that competitively inhibits both LAT1 and LAT2. Large neutral amino acids (L-methionine, L-phenylalanine and L-tyrosine) and BCH inhibited the uptake of both D- and L-isomers of [^{18}F]FMT completely; but L-glycine, a small neutral amino acid, did not inhibit it at all (Fig. 3A). Furthermore, system L is known to be a Na^+-independent amino acid transporter [24,25]. To make clear the character of the transport system, we examined the Na^+ dependency of uptake of D- and L-isomers of [^{18}F]FMT. The uptake of D- and L-isomers of [^{18}F]FMT was not affected by the presence of Na^+ ions (Fig. 3B).

Moreover, the RT-PCR experiment done to determine the expression of the major system L transporters LAT1 and LAT2 and their functional associated protein 4F2hc indicated that both C6 glioma and HeLa cells expressed LAT1 and 4F2hc mRNA but not LAT2 (Fig. 5). These results suggest that the major transporter of system L in C6 glioma and HeLa cells was LAT1. Based on these results taken together, we conclude that both D- and L-isomers of [^{18}F]FMT were transported via LAT1 in C6 glioma and HeLa cells. However, the involvement of other transport systems in the actual or in the other tumors is possible.

The dose-dependent inhibitory effect of BCH on D- or L-isomer of [^{18}F]FMT uptake (Fig. 4A) indicated that there was little difference in the IC_{50} value between D- and L-isomers. Comparison of the inhibitory effect of D and L isomers of leucine on the uptake of FMT showed that the uptake of L-[^{18}F]FMT was inhibited at low concentrations of these isomers (Fig. 4B and C). Under physiological conditions, the concentration of amino acids transported via the system L in the plasma is far higher than 100 μM [34]. These data suggest that both D- and L-isomers of [^{18}F]FMT would be competitively transported by system L transporters.

To develop tumor-detecting agents, it is important to have not only higher accumulation in the tumor but also a lower background. This tumor/normal tissue ratio of accumulation highly influences the contrast obtained. Previous reports indicated that the accumulation of [^{18}F]FMT in tumors evaluated by SUV did not differ between D- and L-isomers during a 60-min post administration, but showed that the tumor/blood ratio was significantly different [32,33]. In the present study, we also observed that the SUV of L-isomer was quite similar to that of the D-isomer in tumor tissue, although the latter was only about one-half of the former in normal tissue. At the time point of 60 min, the tumor/blood ratio of D-[^{18}F]FMT was twice as high as that of the L-isomer [32,33]. A previous report suggested that the L-configuration of amino acids is required for the optimal active reabsorption in the renal tubules [38]. D-Isomer of amino acids might be less reabsorbed and consequently more excreted than that of L-isomer. Therefore, as a result, the contrast imaging of tumors was achieved by D-[^{18}F]FMT.

For in vivo evaluation of D-[^{18}F]FMT, we adopted a mouse xenotransplantation model using human tumor cells as a small-animal model for predicting the accumulation of tumor tracer candidates in human tumor cells. [^{18}F]FDG was accumulated not only in the tumor but also in the brain and in the heart. There was not a large difference between the accumulations of L- and D-[^{18}F]FMT in the tumor. However, the accumulation of the tracer in the normal tissue around the tumor, abdominal, chest and brain region was considerably lower with D-[^{18}F]FMT than with L-[^{18}F]FMT. These results suggest that D-[^{18}F]FMT is more suitable for a tumor-detecting agent.

Finally, we evaluated tumor imaging with D-[^{18}F]FMT by using a rat allograft orthotopic brain tumor model. A current report suggests that there is a significant difference in some pathological and pharmacological features between orthotopic tumor models and ectopic tumor models in rodents [39]. Because the conditions of tissues and the bloodstream around the tumor are important for the evaluation of tumor-imaging agents, we selected a rat orthotopic tumor model. With rats bearing C6 glioma transplanted into their left middle brain, we conducted a small-animal PET experiment using D-[^{18}F]FMT. The positron emitter-labeled tracer was injected via a tail vein. The brain tumor, which could not be detected by [^{18}F]FDG PET due to high background, was imaged by D-[^{18}F]FMT. The region of the tumor and autoradiographic image visualized on tumor slices well correlated with the D-[^{18}F]FMT accumulation imaged by PET. These results suggest that D-[^{18}F]FMT might be a useful tracer for tumor detection.

5. Conclusions

This study demonstrated that the artificial large neutral amino acid FMT was accumulated into tumor cells via amino acid transporters. The LAT1 system L transporter was suggested to be the transporter, at least in C6 glioma and HeLa cells. The uptake, release and exchange of L-[^{18}F]FMT were more affected by a physiological concentration of extracellular amino acids than those of the D-isomer. D-[^{18}F]

FMT gave the high-contrast image of the tumor due to the low background. The utility of D-[^{18}F]FMT was especially demonstrated in the orthotopic brain tumor model. Thus D-[^{18}F]FMT appears promising as a tumor-detecting agent for PET diagnosis.

Acknowledgments

We gratefully acknowledge Mr. Kengo Sato and Mr. Norihiro Harada (Hamamatsu Photonics K.K.) for the synthesis of D- and L-isomers of [^{18}F]FMT.

References

[1] Kubota R, Kubota K, Yamada S, Tada M, Ido T, Tamahashi N. Microautoradiographic study for the differentiation of intratumoral macrophages, granulation tissues and cancer cells by the dynamics of fluorine-18-fluorodeoxyglucose uptake. J Nucl Med 1994;35:104–12.

[2] Ishiwata K, Vaalburg W, Elsinga PH, Paans AM, Woldring MG. Comparison of L-[1-^{11}C]methionine and L-methyl-[^{11}C]methionine for measuring in vivo protein synthesis rates with PET. J Nucl Med 1988; 29:1419–27.

[3] Comar D, Cartron J, Maziere M, Marazano C. Labelling and metabolism of methionine-methyl-^{11}C. Eur J Nucl Med 1976;1:11–4.

[4] Ishiwata K, Vaalburg W, Elsinga PH, Paans AM, Woldring MG. Metabolic studies with L-[1-^{14}C]tyrosine for the investigation of a kinetic model to measure protein synthesis rates with PET. J Nucl Med 1988;29:524–9.

[5] Barrio JR, Keen RE, Ropchan JR, MacDonald NS, Baumgartner FJ, Padgett HC, et al. L-[1-^{11}C]leucine: routine synthesis by enzymatic resolution. J Nucl Med 1983;24:515–21.

[6] Casey DL, Digenis GA, Wesner DA, Washburn LC, Chaney JE, Hayes RL, et al. Preparation and preliminary tissue studies of optically active ^{11}C-D- and L-phenylalanine. Int J Appl Radiat Isot 1981;32:325–30.

[7] Lemaire C, Guillaume M, Christiaens L, Palmer AJ, Cantineau R. A new route for the synthesis of [^{18}F]fluoroaromatic substituted amino acids: no carrier added L-*p*-[^{18}F]fluorophenylalanine. Int J Rad Appl Instrum [A] 1987;38:1033–8.

[8] Coenen HH, Kling P, Stocklin G. Cerebral metabolism of L-[2-^{18}F] fluorotyrosine, a new PET tracer of protein synthesis. J Nucl Med 1989;30:1367–72.

[9] Ishiwata K, Kawamura K, Wang WF, Furumoto S, Kubota K, Pascali C, et al. Evaluation of *O*-[^{11}C]methyl-L-tyrosine and *O*-[^{18}F]fluoromethyl-L-tyrosine as tumor imaging tracers by PET. Nucl Med Biol 2004;31:191–8.

[10] Wester HJ, Herz M, Weber W, Heiss P, Senekowitsch-Schmidtke R, Schwaiger M, et al. Synthesis and radiopharmacology of *O*-(2-[^{18}F] fluoroethyl)-L-tyrosine for tumor imaging. J Nucl Med 1999;40:205–12.

[11] Heiss P, Mayer S, Herz M, Wester HJ, Schwaiger M, Senekowitsch-Schmidtke R. Investigation of transport mechanism and uptake kinetics of *O*-(2-[^{18}F]fluoroethyl)-L-tyrosine in vitro and in vivo. J Nucl Med 1999;40:1367–73.

[12] Tang G, Tang X, Wang M, Luo L, Gan M. Fully automated synthesis of *O*-(3-[^{18}F]fluoropropyl)-L-tyrosine by direct nucleophilic exchange on a quaternary 4-aminopyridinium resin. Appl Radiat Isot 2003;58: 685–9.

[13] Tang G, Wang M, Tang X, Luo L, Gan M. Synthesis and evaluation of *O*-(3-[^{18}F]fluoropropyl)-L-tyrosine as an oncologic PET tracer. Nucl Med Biol 2003;30:733–9.

[14] Ishiwata K, Kasahara C, Hatano K, Ishii S, Senda M. Carbon-11 labeled ethionine and propionine as tumor detecting agents. Ann Nucl Med 1997;11:115–22.

[15] Tamemasa O, Goto R, Takeda A, Maruo K. High uptake of ^{14}C-labeled D-amino acids by various tumors. Gann 1982;73:147–52.

[16] Takeda A, Goto R, Tamemasa O, Chaney JE, Digenis GA. Biological evaluation of radiolabeled D-methionine as a parent compound in potential nuclear imaging. Radioisotopes 1984;33:213–7.

[17] Goto R, Unno K, Takeda A, Okada S, Tamemasa O. Tumor accumulation of D-selenomethionine-75Se in tumor-bearing mice. J Pharmacobiodyn 1987;10:456–61.

[18] Martineau M, Baux G, Mothet JP. D-Serine signalling in the brain: friend and foe. Trends Neurosci 2006;29:481–91.

[19] Long Z, Sekine M, Adachi M, Furuchi T, Imai K, Nimura N, et al. Cell density inversely regulates D- and L-aspartate levels in rat pheochromocytoma MPT1 cells. Arch Biochem Biophys 2002;404: 92–7.

[20] Bendikov I, Nadri C, Amar S, Panizzutti R, De Miranda J, Wolosker H, et al. A CSF and postmortem brain study of D-serine metabolic parameters in schizophrenia. Schizophr Res 2007;90:41–51.

[21] Katsuki H, Nonaka M, Shirakawa H, Kume T, Akaike A. Endogenous D-serine is involved in induction of neuronal death by *N*-methyl-D-aspartate and simulated ischemia in rat cerebrocortical slices. J Pharmacol Exp Therapeut 2004;311:836–44.

[22] Homma H. Biochemistry of D-aspartate in mammalian cells. Amino Acids 2007;32:3–11.

[23] Kanai Y, Endou H. Heterodimeric amino acid transporters: molecular biology and pathological and pharmacological relevance. Curr Drug Metab 2001;2:339–54.

[24] Kanai Y, Segawa H, Miyamoto K, Uchino H, Takeda E, Endou H. Expression cloning and characterization of a transporter for large neutral amino acids activated by the heavy chain of 4F2 antigen (CD98). J Biol Chem 1998;273:23629–32.

[25] Segawa H, Fukasawa Y, Miyamoto K, Takeda E, Endou H, Kanai Y. Identification and functional characterization of a Na^+-independent neutral amino acid transporter with broad substrate selectivity. J Biol Chem 1999;274:19745–51.

[26] Nakamura E, Sato M, Yang H, Miyagawa F, Harasaki M, Tomita K, et al. 4F2 (CD98) heavy chain is associated covalently with an amino acid transporter and controls intracellular trafficking and membrane topology of 4F2 heterodimer. J Biol Chem 1999;274:3009–16.

[27] Kim DK, Kim IJ, Hwang S, Kook JH, Lee MC, Shin BA, et al. System L-amino acid transporters are differently expressed in rat astrocyte and C6 glioma cells. Neurosci Res 2004;50:437–46.

[28] Yanagida O, Kanai Y, Chairoungdua A, Kim DK, Segawa H, Nii T, et al. Human L-type amino acid transporter 1 (LAT1): characterization of function and expression in tumor cell lines. Biochim Biophys Acta 2001;1514:291–302.

[29] Prasad PD, Wang H, Huang W, Kekuda R, Rajan DP, Leibach FH, et al. Human LAT1, a subunit of system L amino acid transporter: molecular cloning and transport function. Biochem Biophys Res Commun 1999; 255:283–8.

[30] Pineda M, Fernandez E, Torrents D, Estevez R, Lopez C, Camps M, et al. Identification of a membrane protein, LAT-2, that co-expresses with 4F2 heavy chain, an L-type amino acid transport activity with broad specificity for small and large zwitterionic amino acids. J Biol Chem 1999;274:19738–44.

[31] Rossier G, Meier C, Bauch C, Summa V, Sordat B, Verrey F, et al. LAT2, a new basolateral 4F2hc/CD98-associated amino acid transporter of kidney and intestine. J Biol Chem 1999;274:34948–54.

[32] Tsukada H, Sato K, Fukumoto D, Kakiuchi T. Evaluation of D-isomers of *O*-^{18}F-fluoromethyl, *O*-^{18}F-fluoroethyl and *O*-^{18}F-fluoropropyl tyrosine as tumour imaging agents in mice. Eur J Nucl Med Mol Imaging 2006;33:1017–24.

[33] Tsukada H, Sato K, Fukumoto D, Nishiyama S, Harada N, Kakiuchi T. Evaluation of D-isomers of *O*-^{11}C-methyl tyrosine and *O*-^{18}F-fluoromethyl tyrosine as tumor-imaging agents in tumor-bearing mice: comparison with L- and D-^{11}C-methionine. J Nucl Med 2006; 47:679–88.

[34] Gitlitz PH, Sunderman Jr FW, Hohnadel DC. Ion-exchange chromatography of amino acids in sweat collected from healthy subjects during sauna bathing. Clin Chem 1974;20:1305–12.

[35] Oberdorfer F, Hull WE, Traving BC, Maier-Borst W. Synthesis and purification of 2-deoxy-2-[^{18}F]fluoro-D-glucose and 2-deoxy-2-[^{18}F]fluoro-D-mannose: characterization of products by ^{1}H- and ^{19}F-NMR spectroscopy. Int J Rad Appl Instrum [A] 1986;37:695–701.

[36] Takeda A, Tamano H, Oku N. Alteration of zinc concentrations in the brain implanted with C6 glioma. Brain Res 2003;965:170–3.

[37] Fernstrom JD, Larin F, Wurtman RJ. Daily variations in the concentrations of individual amino acids in rat plasma. Life Sci Pt 1971;10:813–9.

[38] Williams WM, Huang KC. Structural specificity in the renal tubular transport of tyrosine. J Pharmacol Exp Therapeut 1981;219:69–74.

[39] Kubota T. Metastatic models of human cancer xenografted in the nude mouse: the importance of orthotopic transplantation. J Cell Biochem 1994;56:4–8.

Journal of the American College of Cardiology
© 2009 by the American College of Cardiology Foundation
Published by Elsevier Inc.

Vol. 53, No. 8, 2009
ISSN 0735-1097/09/$36.00
doi:10.1016/j.jacc.2008.11.014

PRE-CLINICAL RESEARCH

Prolonged Targeting of Ischemic/Reperfused Myocardium by Liposomal Adenosine Augments Cardioprotection in Rats

Hiroyuki Takahama, MD,*†‡ Tetsuo Minamino, MD, PHD,§ Hiroshi Asanuma, MD, PHD,† Masashi Fujita, MD, PHD,§ Tomohiro Asai, PHD,¶ Masakatsu Wakeno, MD, PHD,*†‡ Hideyuki Sasaki, MD,*†‡ Hiroshi Kikuchi, PHD,# Kouichi Hashimoto,** Naoto Oku, PHD,¶ Masanori Asakura, MD, PHD,† Jiyoong Kim, MD,† Seiji Takashima, MD, PHD,§ Kazuo Komamura, MD, PHD,‖ Masaru Sugimachi, MD, PHD,‖ Naoki Mochizuki, MD, PHD,*‡ Masafumi Kitakaze, MD, PHD, FACC†

Osaka, Shizuoka, and Tokyo, Japan

Objectives The purpose of this study was to investigate whether liposomal adenosine has stronger cardioprotective effects and fewer side effects than free adenosine.

Background Liposomes are nanoparticles that can deliver various agents to target tissues and delay degradation of these agents. Liposomes coated with polyethylene glycol (PEG) prolong the residence time of drugs in the blood. Although adenosine reduces the myocardial infarct (MI) size in clinical trials, it also causes hypotension and bradycardia.

Methods We prepared PEGylated liposomal adenosine (mean diameter 134 ± 21 nm) by the hydration method. In rats, we evaluated the myocardial accumulation of liposomes and MI size at 3 h after 30 min of ischemia followed by reperfusion.

Results The electron microscopy and ex vivo bioluminescence imaging showed the specific accumulation of liposomes in ischemic/reperfused myocardium. Investigation of radioisotope-labeled adenosine encapsulated in PEGylated liposomes revealed a prolonged blood residence time. An intravenous infusion of PEGylated liposomal adenosine (450 μg/kg/min) had a weaker effect on blood pressure and heart rate than the corresponding dose of free adenosine. An intravenous infusion of PEGylated liposomal adenosine (450 μg/kg/min) for 10 min from 5 min before the onset of reperfusion significantly reduced MI size (29.5 ± 6.5%) compared with an infusion of saline (53.2 ± 3.5%, $p < 0.05$). The antagonist of adenosine A_1, A_{2a}, A_{2b}, or A_3 subtype receptor blocked cardioprotection observed in the PEGylated liposomal adenosine-treated group.

Conclusions An infusion as PEGylated liposomes augmented the cardioprotective effects of adenosine against ischemia/reperfusion injury and reduced its unfavorable hemodynamic effects. Liposomes are promising for developing new treatments for acute MI. (J Am Coll Cardiol 2009;53:709–17) © 2009 by the American College of Cardiology Foundation

Liposomes are now widely used for drug delivery in cancer treatment to target specific organs actively or passively and to prevent the degradation of chemotherapy agents (1). However, the application of liposomes for cardiovascular diseases is still limited. In ischemic/reperfused myocardium, cellular permeability is enhanced and vascular endothelial integrity is disrupted (2,3), suggesting that nanoparticles

See page 718

*From the Department of Molecular Imaging in Cardiovascular Medicine, Osaka University Graduate School of Medicine, Osaka, Japan; †Department of Cardiovascular Medicine, National Cardiovascular Center, Osaka, Japan; ‡Department of Structural Analysis, Research Institute, National Cardiovascular Center, Osaka, Japan; §Department of Cardiovascular Medicine, Osaka University Graduate School of Medicine, Osaka, Japan; ‖Department of Cardiovascular Dynamics, Research Institute, National Cardiovascular Center, Osaka, Japan; ¶Department of Medical Biochemistry, School of Pharmaceutical Sciences, University of Shizuoka, Shizuoka, Japan; #Daiichi Pharmaceutical Co., Tokyo, Japan; and the **Daiichi-Sankyo Pharmaceutical Co., Tokyo, Japan. Supported by a grant for Scientific Research and a grant for the Advancement of Medical Equipment from the Japanese Ministry of Health, Labor, and Welfare, as well as a grant from the Japan Cardiovascular Research Foundation.

Manuscript received September 4, 2008; revised manuscript received October 21, 2008, accepted November 3, 2008.